Effect of Kilo-Tesla Magnetic Fields on Ignition and Burn Dynamics in Fast Ignition Laser Fusion*)

Naoki MATSUMURA[1)], Tomoyuki JOHZAKI[1,2)], Wookyung KIM[1)] and Takuma ENDO[1)]

[1)]*Graduate School of Advanced Science and Engineering, Hiroshima University, Higashi-Hiroshima 739-8527, Japan*

[2)]*Institute of Laser Engineering, Osaka University, Suita 565-0871, Japan*

(Received 8 January 2023 / Accepted 7 June 2023)

In fast ignition laser fusion, electron beam guiding with a kilo-tesla magnetic field has been proposed to avoid divergence of the beam, which significantly enhances the core heating efficiency. In addition to beam guiding, magnetic fields affect electron heat conduction and alpha particle energy transport. The objective of this study is to estimate the effect of a magnetic field on ignition and burn propagation dynamics of a high-gain target in fast ignition (FI) laser fusion based on axially symmetric two-dimensional burn simulations. A uniformly compressed DT plasma sphere with a cylindrical hot spot was assumed as the initial condition. A magnetic field of 100 kT was applied along the symmetrical axis. In the ignition phase, the suppression of the alpha particle flux and heat conduction by the magnetic field fastens temperature rise in the hot spot. However, the magnetic field reduced the burn propagation speed and then increased the burning time, which enhanced the erosion of the fuel edge by rarefaction waves and decreased the effective areal density of the fuel. Consequently, the burnup fraction for a 100 kT magnetic field was 11% lower than that without a magnetic field.

Keywords: fast ignition, laser fusion, alpha particle transport, electron heat conduction, kilo-tesla magnetic field, radiation-hydro simulation

DOI: 10.1585/pfr.18.2404061

1. Introduction

Fast ignition (FI) laser fusion [1], in which the edge of a compressed fuel is heated by a laser-produced electron beam to the ignition temperature, is an alternative approach to central spark ignition (CSI) scheme [2]. Compared with CSI, the requirement for spherical symmetry for implosion is relaxed because the hot spot does not need to be formed by implosion. In addition, FI, in which the fuel is isochorically compressed, can achieve an areal density equivalent to that of an isobarically compressed fuel in CSI with a small fuel mass. Therefore, FI can achieve the same burnup fraction as CSI with low implosion energy.

One of the critical issues in FI laser fusion is the large divergence of the laser-produced electron beam, which inhibits effective core heating. To solve this problem, electron-beam guiding using a kilo-tesla-class magnetic field has been proposed [3]. The improvement in the heating efficiency by this guiding scheme has been demonstrated by numerical simulations [4, 5] and experiment using the GEKKO-LFEX laser system at ILE Osaka University [6]. In the experiment, a kilo-tesla-class magnetic field was applied using a capacitor coil target [7], and the magnetic field strength reached about 0.6 kT [8].

The magnetic field also affects ignition and burn dynamics through the suppression of electron heat conduction and alpha particle transport in the direction perpendicular to the magnetic field. The simulation of CSI for an NIF experiment showed that a kilo-tesla class magnetic field was formed by compressing a 50 T seed field through fuel implosion, which resulted in relaxing ignition criterion [9]. This is because the range of alpha particles was reduced by the magnetic field, and then the self-heating rate in a hot spot was enhanced. In addition, the electron heat conduction was suppressed perpendicular to the magnetic field. Suppression of the energy flux from the hot spot to the main fuel relaxed the ignition criterion. However, in the burn propagation phase, the magnetic field reduces the energy flux of alpha particles and electron heat conduction from the burning area to the unburned main fuel, resulting in the suppression of burn propagation [10, 11].

Figure 1 shows (a) the ratio of path length λ_α and Larmor radius $r_{L\alpha}$ of a 3.5 MeV alpha particle Ω_α, and (b) electron hall parameter Ω_e in DT plasma ($\rho = 300\,\mathrm{g/cm^3}$). The effect of the magnetic field appears in the areas of $\Omega_\alpha \gtrsim 1$ and $\Omega_e \gtrsim 1$. The range of the alpha particle is limited to within the Larmor radius under a strong magnetic field. The collisional range determined by the Coulomb interaction increases with increasing plasma temperature. This implies that for a given magnetic field strength, the effect of the magnetic field becomes pronounced in high-temperature plasma. Similarly, in the case of electron

author's e-mail: tjohzaki@hiroshima-u.ac.jp

*) This article is based on the presentation at the 31st International Toki Conference on Plasma and Fusion Research (ITC31).

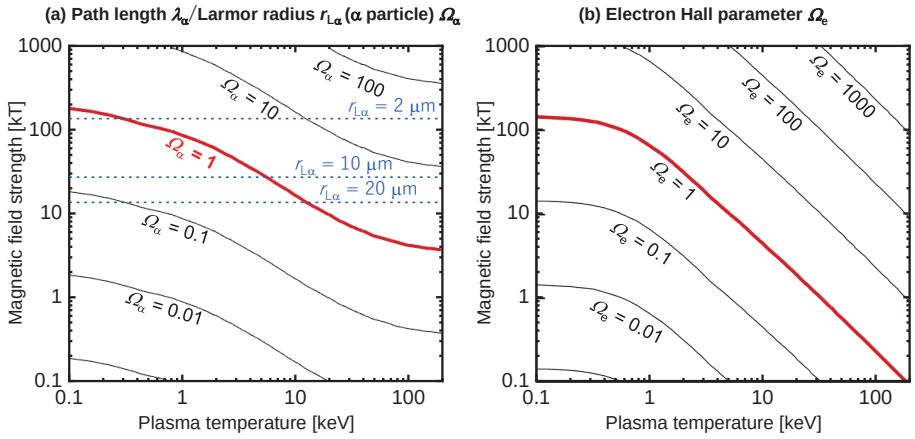

Fig. 1 (a) Ratio of path length λ_α to Larmor radius $r_{L\alpha}$ of a 3.5 MeV alpha particle Ω_α and (b) electron Hall parameter Ω_e (ρ = 300 g/cm^3, D:T = 1:1) in plasma temperature and magnetic field strength plane. Path length of alpha particle is the flight distance of alpha particle along its trajectory until thermalization. The blue broken lines in (a) indicate $r_{L\alpha}$.

heat conduction, the effect of the magnetic field becomes stronger as the electron Hall parameter increases with the temperature for a given magnetic field strength.

In the ignition phase of FI, typical hot spot radius and temperature are 20 μm and 10 keV, respectively. For magnetic field strength $B \gtrsim 20$ kT, the Larmor radius of the alpha particle is less than the hot spot radius. Therefore, the alpha-particle heating rate in the hot spot increases, which may relax the ignition condition.

In the burn propagation phase, energy transport due to electron heat conduction and alpha particles from the burning region (several tens to 100 keV) to the unburned region (~0.1 keV), which is the so-called preheating in front of the burn wave, plays an important role in burn propagation. For $B \gtrsim 100$ kT, energy transport in the direction perpendicular to the magnetic field is strongly suppressed, which will affect burn propagation.

In FI, a kilo-tesla-class magnetic field is required at the fast electron generation point for electron beam guiding [12]. This applied magnetic field is further compressed during fuel implosion. For instance, Knauer et al. [13] showed about a thousand times compression of a seed field through implosion. In the case of electron beam guiding, an externally applied kilo-tesla-class magnetic field is expected to be compressed up to several tens to 100 kT in the high-density fuel region through the implosion of a high-gain target, where the fuel is compressed up to thousands times of the solid density. The ignition and burn dynamics in FI, where a fusion reaction is ignited at the edge of an isochorically compressed fuel under an extremely strong magnetic field, have not yet been investigated.

The objective of this study is to estimate the magnetic field effects through the suppression of electron heat conduction and alpha particle transport on burn dynamics and the resultant burnup fraction in FI laser fusion. In Section 2, we briefly explain the hybrid code, FIBMET, and the simulation setup. The simulation results and discussion are presented in Section 3, in which the effects of the suppression of electron heat conduction and alpha particle transport on ignition and burn dynamics in the presence of a magnetic field are discussed. Finally, a summary is provided in Section 4.

2. Simulation Setup

We conducted burn simulations using the axial symmetric two-dimensional (2D) simulation code "FIBMET" [14] which is based on an Eulerian radiation-hydro code. In this code, the plasma is treated as a one-fluid two-temperature model, and QEOS [15] was used for the equations of state. The electron heat conduction was calculated using a flux-limited diffusion model with the Ji-Held diffusion coefficient [16] which considers the magnetic field effect. The alpha particle transport was calculated using the particle method which considers collisions with plasma particles and the Lorentz force. The Li-Petrasso model [17] was used for stopping power. The temporal evolution of the magnetic field was calculated using the MOC-CT scheme [18]. The radiation transport was calculated using a flux-limited multi-group diffusion model where only a free-free process was considered.

Figure 2 shows the simulation setup. For the initial condition, we assumed a spherical isochoric DT fuel (D:T = 1:1) with a cylindrical hot spot at the fuel edge. The densities of the main fuel and hot spot were equal ($\rho_f = \rho_h$ = 300 g/cm^3). The isentrope parameter of the main fuel was set as $\alpha_f = 2$, the corresponding temperature T_f was 0.16 keV, and the main fuel areal density ρR_f was 3.0 g/cm^2. For the hot spot, we assumed that the temperature T_h was 6 keV, the radius r_h was 20 μm, and the areal density along the axial direction ρL_h was 2.0 g/cm^2. For the fuel, the uniform magnetic field, B_0 = 0 or 100 kT, was initially applied in the direction of the symmetric axis.

3. Results and Discussion

Figure 3 shows the temporal evolution of the DT reaction rate for $B_0 = 0$ and 100 kT. In the ignition phase, the reaction rate when $B_0 = 100$ kT was higher than that when $B_0 = 0$ kT. In contrast, in the burn propagation phase, the increase in the reaction rate was slower for $B_0 = 100$ kT. The burnup fraction for $B_0 = 100$ kT was 0.27, which was 11% lower than that for $B_0 = 0$ kT. The reasons for these results are discussed as follows.

Figure 4 shows the spatial profiles of (a) ion temperature T_i, (b) electron conduction heating rate q_e, (c) alpha-particle heating rate q_α, and (d) DT reaction rate β in the ignition phase ($t = 15$ ps). The electron heat flux in the r direction around the boundary between the hot spot and main fuel was suppressed, and the energy loss from the hot spot was reduced. Additionally, the suppression of alpha particle transport perpendicular to the magnetic field increased the alpha particle heating rate in the region around the z axis. Consequently, the temperature in the hot spot and the reaction rate increased. This effect is expected to reduce the core heating energy required for ignition.

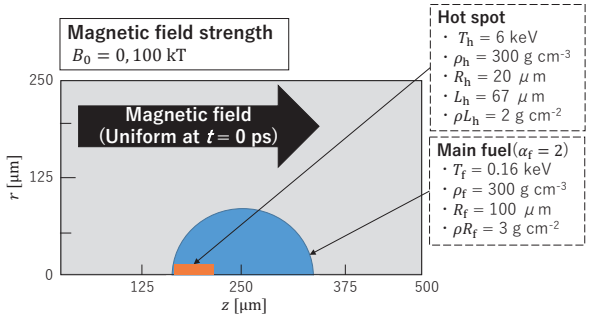

Fig. 2 Initial condition of FI laser fusion simulation.

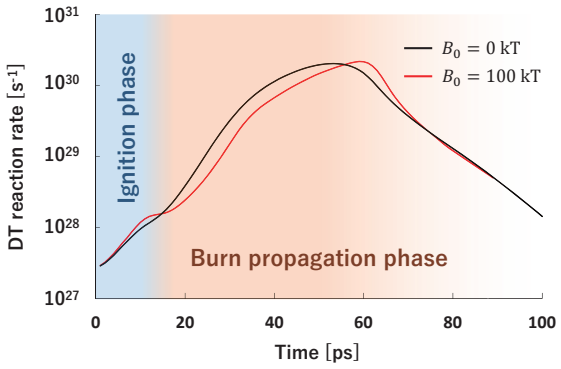

Fig. 3 Temporal evolution of DT reaction rates for $B_0 = 0$ and 100 kT.

In contrast to the suppression of energy transport in r direction with a magnetic field, q_e and q_α along the magnetic field were increased by increasing the temperature in the hot spot. This results in enhancing the heating rates at the boundary between the hot spot and the main fuel in the z direction. Hence, the magnetic field suppressed burn propagation in the r direction and enhanced propagation in the z direction.

Figure 5 shows the (a) 2D spatial profile of β and (b) one-dimensional (1D) profiles of ρ, q_e, q_α, T_i, electron temperature T_e, and source power of alpha-particle s_α. The 1D profiles were plotted along the arrows shown in Fig. 5 (a). In this phase, the burn wave propagates with the shock wave. Without a magnetic field, the alpha particles and electron conduction diffusively heated around the shock wave. In particular, electron conduction heated strongly in front of the shock wave and increased the electron temperature, which extended the range of alpha particles. With a magnetic field, the transport of alpha particles and bulk electrons was strongly suppressed in the direction perpendicular to the magnetic field. Thus, preheating by alpha particles and electron heat conduction in front of the shock wave was suppressed, which reduced the propagation speed of the burn wave. In addition, since the temperature behind the shock wave was higher than that without a magnetic field, the fuel behind the shock wave expanded faster and then the density decreased faster. Thus,

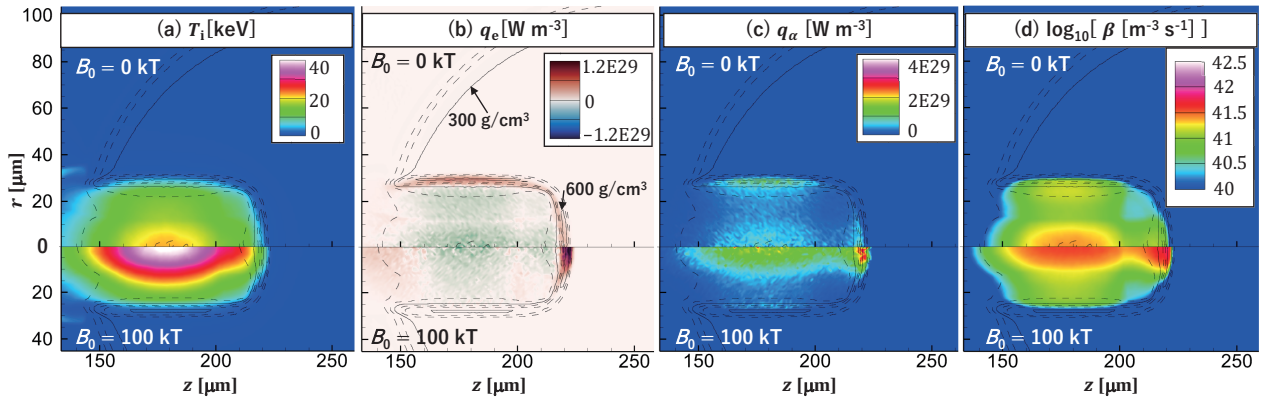

Fig. 4 Spatial profiles of (a) ion temperature T_i, heating rates by (b) electron conduction q_e, (c) alpha-particle q_α, and (d) DT reaction rate β at $t = 15$ ps (ignition phase). The negative value of q_e indicates energy loss rate. The lines indicate density contours every 100 g/cm^3.

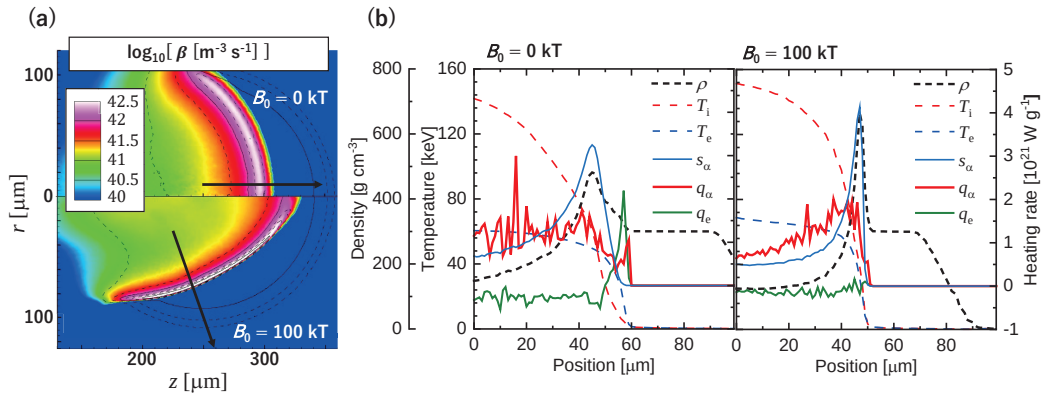

Fig. 5 (a) 2D spatial profiles of DT reaction rate β and (b) 1D profiles of ρ, q_e, q_α, T_i, electron temperature T_e, and source power of alpha-particle s_α at $t = 50$ ps (burn propagation phase). 1D spatial profiles show the profiles along the arrows in (a). A negative value of q_e indicates energy loss rate. The lines in (a) indicate density contours every 100 g/cm^3.

the profiles of ρ and temperature around the shock wave were steepened and the reaction zone was narrowed.

The decreasing propagation speed of the burn wave delayed the time required for it to reach the outer edge of the fuel. During burn propagation, the size of the high-density fuel decreased because of entering rarefaction wave from the fuel outer edge. Thus, the effective areal density decreased. Consequently, even though the peak value of DT reaction rate did not differ between the two cases (Fig. 1), the burnup fraction when $B_0 = 100$ kT decreased by 11 % compared with that when $B_0 = 0$ kT.

4. Summary

We conducted 2D FI burn simulations to evaluate the effect of magnetic field on ignition and burn propagation dynamics in FI laser fusion. For the initial condition, we assumed a uniformly compressed DT fuel with a cylindrical hot spot and a uniformly applied magnetic field along the symmetric axis.

In the ignition phase, the suppression of alpha particle flux and electron heat conduction by the magnetic field increased the temperature and reaction rate in the hot spot. This may reduce the externally injected energy required for ignition. However, in the burn propagation phase, the magnetic field reduced the reaction zone thickness and burn propagation speed because of the suppression of preheating in front of the burn wave. The lower burn propagation speed increased the burn time, which allowed the rarefaction wave to enter the fuel more deeply from the outside during the burn time, thereby reducing the effective areal density and decreasing the burnup fraction.

Electron-beam guiding requires a magnetic field of several kilo teslas. In contrast, the results of this study showed that an excessively high-intensity magnetic field negatively affected burn propagation. In addition, the external magnetic field affected the implosion process, and the compressed magnetic field had a complex structure [19]. It is necessary to evaluate and optimize the overall characteristics of magnetic-field-assisted fast ignition by integrated simulation that considers the process from implosion to formation of a hot spot.

Acknowledgements

This work was supported by JSPS KAKENHI (grant numbers JP20H01886 and JP 22H00118) and the NIFS Collaboration Research program (NIFS12KUGK057, NIFS21KUGK138).

[1] M. Tabak *et al.*, Phys. Plasmas **1**, 1626 (1994).
[2] J. Nuckolls *et al.*, Nature **239**, 139 (1972).
[3] D.J. Strozzi *et al.*, Phys. Plasmas **19**, 072711 (2012).
[4] H. Nagatomo *et al.*, Nucl. Fusion **57**, 086009 (2017).
[5] T. Johzaki *et al.*, Plasma Phys. Control. Fusion **59**, 014045 (2017).
[6] S. Sakata *et al.*, Nat. Commun. **9**, 3937 (2018).
[7] H. Daido *et al.*, Phys. Rev. Lett. **56**, 846 (1986).
[8] K.F.F. Law *et al.*, Appl. Phys. Lett. **108**, 091104 (2016).
[9] C.A. Walsh *et al.*, Phys. Plasmas **26**, 022701 (2019).
[10] S.A. Slutz and R.A. Vesey, Phys. Rev. Lett. **108**, 025003 (2012).
[11] B. Appelbe *et al.*, Phys. Plasmas **28**, 032705 (2021).
[12] T. Johzaki *et al.*, High Energy Density Phys. **36**, 100841 (2020).
[13] J.P. Knauer *et al.*, Phys. Plasmas **17**, 056318 (2010).
[14] T. Johzaki *et al.*, J. Phys. IV France **133**, 385 (2006).
[15] R.M. More *et al.*, Phys. Fluids **31**, 3059 (1988).
[16] J. Young Ji and E.D. Held, Phys. Plasmas **20**, 042114 (2013).
[17] C. Li and R.D. Petrasso, Phys. Rev. Lett. **70**, 3059 (1993), Erratum-ibid. **114** 199901 (2015).
[18] J.F. Hawley and J.M. Stone, Comput. Phys. Commun. **89**, 127 (1995).
[19] H. Nagatomo *et al.*, Nucl. Fusion **55**, 093028 (2015).